

Response of a  $\text{PbWO}_4$ -Scintillator Array to Electrons in the Energy Regime Below 1 GeV<sup>1</sup>

R. Novotny, W. Döring, K. Mengel, and V. Metag

II. Physics Institute, University of Giessen, Germany

C. Pienne

University of Clermont-Ferrand, France

**Abstract**

$\text{PbWO}_4$  has been selected as the most appropriate scintillator material for future calorimeter projects at LHC to detect high energy photons in the multiple GeV range. In spite of the low yield of scintillation light, the applicability of the scintillator to detect photons and particles at energies well below 1 GeV has been studied using monoenergetic electrons between 180 and 855 MeV. The individual crystals ( $20 \times 20 \times 150 \text{ mm}^3$ ) are characterized by the optical quality and the response to low energy  $\gamma$ -sources using hybrid photo diode tubes. The energy resolution of the EM-shower deposited by electrons in a  $3 \times 3$  crystal matrix amounts to  $\sigma/E = 2.39\%/\sqrt{E} + 0.20\%$  ( $E$  given in GeV). The obtained time resolution of  $\sigma \leq 130$  ps allows photon/particle discrimination via time-of-flight measurement.

**I. INTRODUCTION**

The calorimetry at relativistic heavy ion collisions concentrates primarily on the detection of photons of energies near or far below 1 GeV. Operating photon detectors such as the  $\text{BaF}_2$ -spectrometer TAPS [1] combine high energy resolution with efficient photon/particle discrimination capabilities due to the fast response and particle selective pulse shape of the scintillator.  $\text{PbWO}_4$  has been rediscovered recently [2,3,4,5,6] as a very attractive, fast, dense and highly radiation resistant inorganic scintillator material suitable for large scale industrial production for new generation high energy homogeneous calorimeters as to be constructed for the CMS or ALICE detectors for LHC [7,8]. Table 1 summarizes the relevant physical properties of the scintillator  $\text{PbWO}_4$ .

Table 1  
The relevant physical properties of  $\text{PbWO}_4$

Physical properties	
density $\rho$ [ $\text{g/cm}^3$ ]	8.28
index of refraction (at $\lambda=632\text{nm}$ )	2.16
radiation length $X_0$ [cm]	0.89
Molière radius $R_M$ [cm]	2.0
major decay constants [ns]	$\leq 10, -40$
peak wavelength of emission [nm]	450 - 500
temperature dependence of light yield [ $\%/^\circ\text{C}$ ]	-1.9

<sup>1</sup> supported by Bundesministerium für Bildung, Wissenschaft, Forschung und Technologie (BMBF)

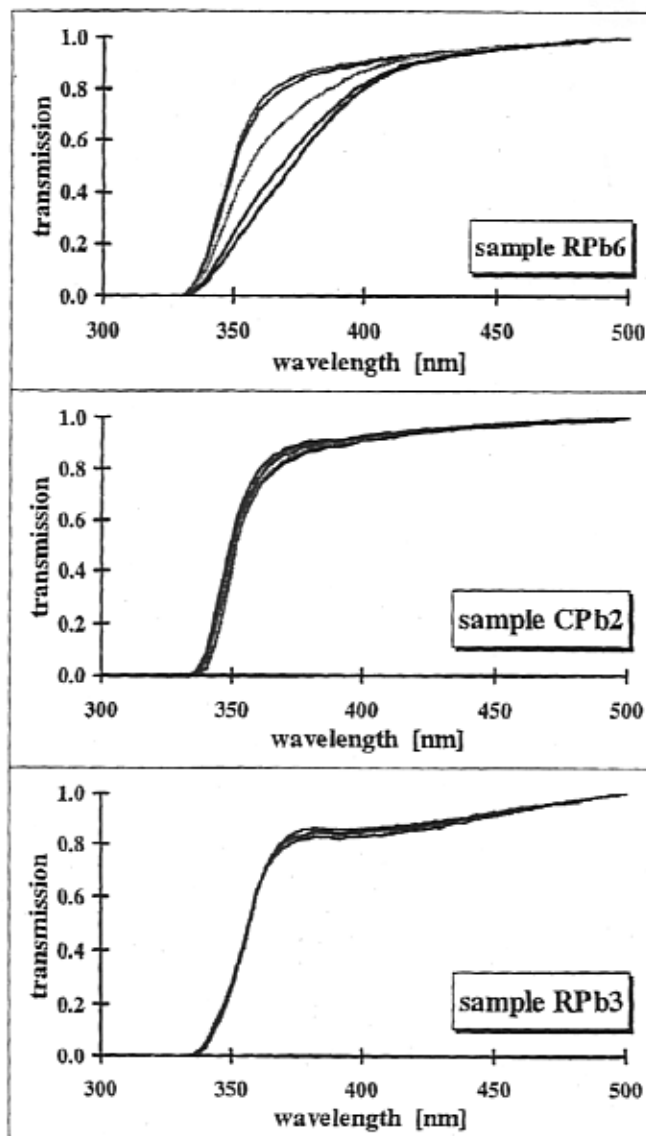


Figure 1: Measured optical performance of three selected  $\text{PbWO}_4$  samples. The transmission has been measured perpendicular to the longitudinal axis of the crystal (thickness  $d = 20$  mm) at different positions. The measured values are normalized to  $t = 100\%$  at  $\lambda = 500$  nm.

The extremely low values of radiation length and Molière radius, respectively, allow the design of a very compact detector system. However, due to the thermal quenching at

room temperature, one has to cope with a very fast but low yield of scintillation light. Therefore, the applicability as a radiation detector at energies even far below 1 GeV has to be investigated experimentally. Inspired by the ongoing experimental program of the TAPS collaboration we have initiated an extensive test program to evaluate the scintillator properties of  $\text{PbWO}_4$  with respect to the special needs in medium and relativistic heavy ion collisions or photonuclear reactions.

In the following section the crystal samples available to us will be classified by the optical transparency and homogeneity. The luminescence yield can be measured directly even with low energy  $\gamma$ -sources by exploiting the excellent single photoelectron resolution of hybrid photo diode tubes (HPD). The experimental measurement of the response function of a  $3 \times 3$  crystal matrix to electrons between 180 and 855 MeV will be reported in the third chapter. The achieved energy and time resolutions will be discussed in comparison to GEANT3 simulations in the consecutive chapter. The overall performance and future perspectives are concluded in the summary.

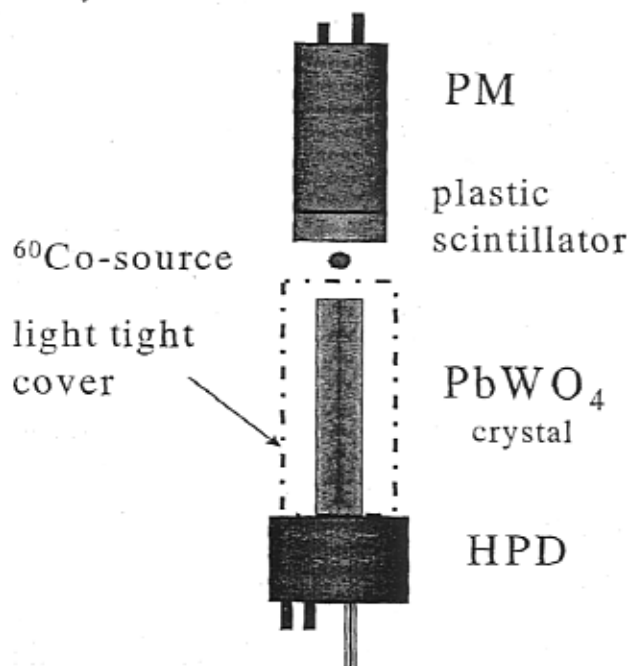


Figure 2: Schematic set-up to determine the luminescence yield using a HPD. The response to low energy  $\gamma$ -rays ( $^{60}\text{Co}$ ) is measured in coincidence with a plastic scintillator.

## II. THE QUALITY OF THE $\text{PbWO}_4$ -CRYSTALS

### A. The Crystal Samples

The performed crystal tests are based on 28 samples with a constant quadrate diameter ( $20 \times 20 \text{ mm}^2$ ) and a length between 150 and 201 mm corresponding to 16 to  $23X_0$ , respectively. The scintillators have been provided by suppliers from Belarus [9] and China [10]. Unfortunately, we do not have details on the production process of each crystal available. All crystal

surfaces are optically polished, but some samples show minor cracks.

### B. The Optical Transparency

The optical transparency has been determined within the relevant wavelength regime between 300 and 700 nm using a double beam UV-photo-spectrometer. The crystals are scanned perpendicular to the longitudinal axis in steps of typically 20 mm in order to investigate the homogeneity as well. Fig. 1 shows measured transmission spectra (material thickness  $d = 20 \text{ mm}$ ) taken at 7 equidistant positions along the axis. The distributions have been normalized to a transmission value  $t = 100\%$  at the wavelength  $\lambda = 500 \text{ nm}$  for better comparison. Absolute values obtained at that wavelength vary between 79% and 82%. The shown examples represent three typical classes of crystals.

In general, the transmission drops typically to a value of  $t = 50\%$  at a wavelength between 345 and 375 nm. The steepness of the absorption edge can be expressed by the difference of the corresponding wavelengths at transmission values of  $t = 30\%$  and  $70\%$ , respectively, ( $\Delta\lambda = \lambda_{70\%} - \lambda_{30\%}$ ). The parameter  $\Delta\lambda$  varies between 10 and 30 nm. The spectral shape of the optical transmission of several samples indicates (see Fig. 1 (bottom)) a strong, but very broad absorption region between 380 and 440 nm. A fraction of  $\sim 20\%$  of the investigated crystals shows a strong inhomogeneity of the optical quality as illustrated in Fig. 1 (top).

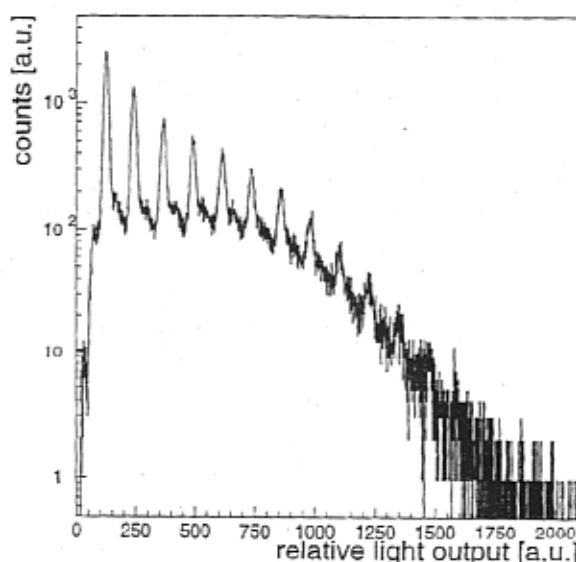


Figure 3: Response of a  $\text{PbWO}_4$  crystal to a  $^{60}\text{Co}$   $\gamma$ -source measured with a hybrid photo diode tube (sample # RPB4).

### C. The Luminescence Yield

The use of low energy  $\gamma$ -sources to study the performance of scintillators represents a very common and convenient test procedure. Unfortunately,  $\text{PbWO}_4$  emits only a few scintillation photons per MeV of deposited energy. Exploiting

the excellent single photoelectron response and resolution of a recently reinvented hybrid photo diode tube (HPD) [11,12,13] - which is a vacuum tube with a photocathode coupled to a silicon PIN diode - allows the use of a  $^{60}\text{Co}$   $\gamma$ -source ( $E_\gamma = 1.17, 1.33$  MeV) in coincident operation with a plastic scintillator as shown schematically in Fig. 2.

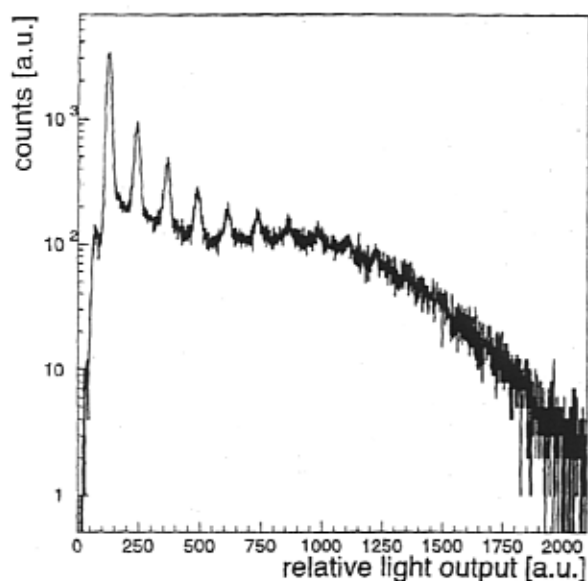


Figure 4: Response of a  $\text{PbWO}_4$  crystal to a  $^{60}\text{Co}$   $\gamma$ -source measured with a hybrid photo diode tube (sample # CPb2).

All crystals have been measured twice by attaching both end surfaces to the photosensor. Fig. 3 illustrates a typical spectrum of the light output. The measured yield is shown on a logarithmic scale. The number of detected photoelectrons (PE) can be counted directly due to the fully linear response. Fig. 4 shows for comparison the distribution measured for one of the crystals with the highest observed photon yield (sample provided by SICCAS), which indicates in addition a different overall shape caused by the different structures due to photopeak and Compton continuum. Figs. 5 and 6 summarize the calculated mean number of PEs of all samples as well as the homogeneity in light collection which is quantified by the difference of the values of PEs determined at both end faces of the crystal, respectively. The scintillators provided by the two suppliers are marked differently.

The wide distribution of the measured light output (LO) reflects the variation of crystal quality as observed in the optical transmission before. Due to the limited number of investigated samples no clear correlations can be established yet. The light-output of  $\text{LO} = 3.4$  photo-electrons for the majority of samples corresponds to  $\sim 120$  photons per MeV of deposited energy, if one takes into account an absorption length of the scintillation light ( $\Lambda = 39$  cm at  $\lambda = 480$  nm, light path  $\sim 30$  cm), a coverage of 64% of the crystal end face by the entrance window of the photosensor, a photocathode quantum efficiency of  $\text{QE} = 14\%$  ( $\lambda = 480$  nm) and an average deposited photon energy of 690 keV (taken from the measured

$^{60}\text{Co}$  spectrum). The four crystals produced in China provide the highest LO but accompanied with the largest inhomogeneity (see Fig. 6). However, one has to consider that these scintillators are also slightly longer (160 to 201 mm). By coupling the best crystal sample to a 2-inch photomultiplier tube (Hamamatsu R2059-01), photopeak energy resolutions of  $\sigma/E = 43\%$  and  $35\%$  have been obtained for  $^{137}\text{Cs}$  ( $E_\gamma = 662$  keV) and  $^{60}\text{Co}$  ( $E_\gamma \sim 1.25$  MeV)  $\gamma$ -sources, respectively.

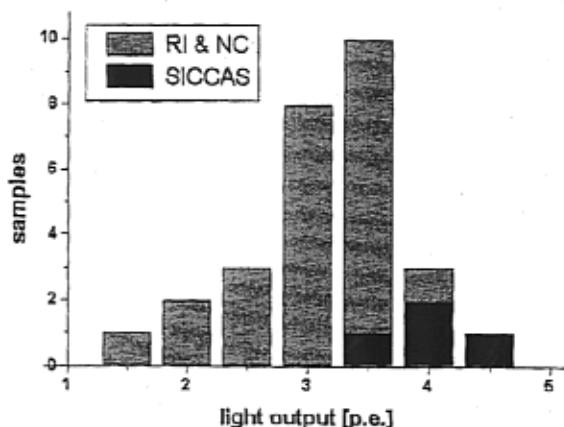


Figure 5: Distribution of the mean number of photo-electrons of all tested crystals measured with a HPD using a  $^{60}\text{Co}$   $\gamma$ -source. The samples of the two different suppliers are marked separately.

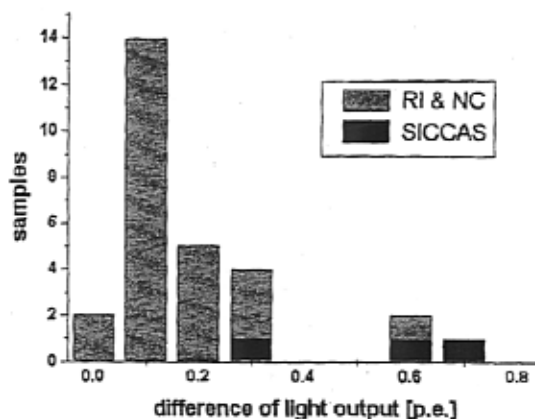


Figure 6: Distribution of the difference of the number of photo-electrons measured separately at both end faces of the crystal. The results are obtained with a HPD using a  $^{60}\text{Co}$   $\gamma$ -source.

### III. THE RESPONSE TO ELECTRONS

#### A. The Experimental Set-up

A matrix consisting of  $3 \times 3$  not preselected crystals has been set up to measure the response function to electrons exploiting the direct beam at the accelerator facility MAMI (University Mainz, Germany [14]). The crystals individually wrapped in TEFLON foil are coupled with optical grease (BAYSILONE 300.000) to photomultiplier tubes (Philips

XP1911) and stacked into a light tight box which can be cooled down to a temperature of  $T \geq 2.5^\circ\text{C}$ . During a typical data taking cycle of a few hours the temperature can be well stabilized ( $\Delta T < 0.2^\circ\text{C}$ ), but a small temperature gradient ( $< 2^\circ\text{C}$ ) within the  $\text{PbWO}_4$  block remains due to the low heat conductivity. Fig. 7 illustrates schematically the experimental set-up including a cross made out of quadrature scintillating fibers ( $2 \times 2 \text{ mm}^2$ , Bicron BCF-12) placed in front of the calorimeter module. The triple coincidence between the pair of fibers and the responding  $\text{PbWO}_4$ -array defines the point of impact. The crystal matrix can be moved by remote control in two dimensions relative to the fiber cross to hit each crystal directly with the beam. That allows to deduce the relative calibration of the matrix components under beam conditions.

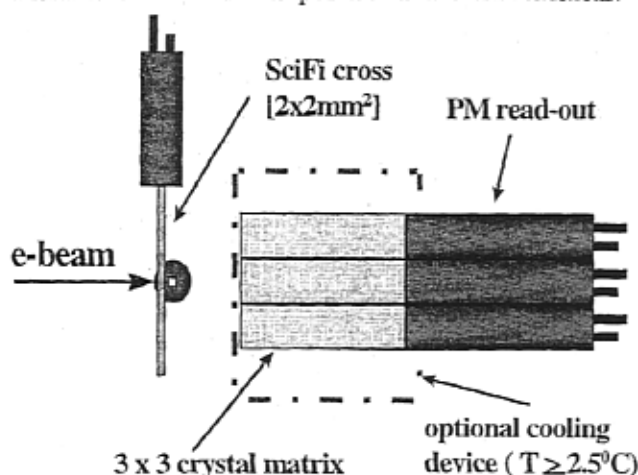


Figure 7: Experimental set-up to study the response function to electrons of a  $3 \times 3$  matrix of  $\text{PbWO}_4$  at MAMI, Mainz.

The individual detector signals have to be transferred via long coaxial cables ( $\sim 100 \text{ m}$ ) to the data acquisition system and are digitized by means of a charge-sensitive ADC (LeCroy 2249W) using different effective integration widths (IW) of 60, 100, 140 or 220 ns. A timing signal deduced by a constant-fraction discriminator (GANELEC FCC8) allows to determine the response time relative to the central module. The energy and time informations of each scintillator including the fiber cross are recorded event-by-event on exabyte tape for an off-line analysis.

The experiment has been performed using electrons of  $E_e = 180, 450$  and  $855 \text{ MeV}$ . The very small momentum spread of the direct beam can be neglected in the further analysis. The crystal matrix was cooled down to  $T = 2.5^\circ\text{C}$ , monitored at the outer surface of the detector array. At the highest energy, the response measurement has been repeated also at room temperature ( $T = 20^\circ\text{C}$ ). In order to minimize pile-up events, the tests have been performed at a coincidence rate of approximately 5000 counts per second.

### B. The Reconstruction of the EM Shower

Each crystal has been hit in the center by the electron beam (spot size  $\sim 2 \times 2 \text{ mm}^2$  as defined by the fiber cross). The response determined for each integration gate including the pedestal of the ADC provide the relative calibration of the

detector matrix to reconstruct the total deposited energy of the EM-shower. Fig. 8 illustrates the shower distribution observed in the individual modules at the highest studied energy of  $E_e = 855 \text{ MeV}$  (IW = 140 ns,  $T = 2.5^\circ\text{C}$ ). At this projectile energy a fraction of 76% of the energy absorbed in total is deposited into the central module as shown in Fig. 9 in comparison to the overall matrix response. The reference for the absolute calibration has been taken from GEANT3 simulations (see next chapter). From the lower part of Fig. 9 an excellent energy resolution of  $\sigma/E = 2.79\%$  can be deduced.

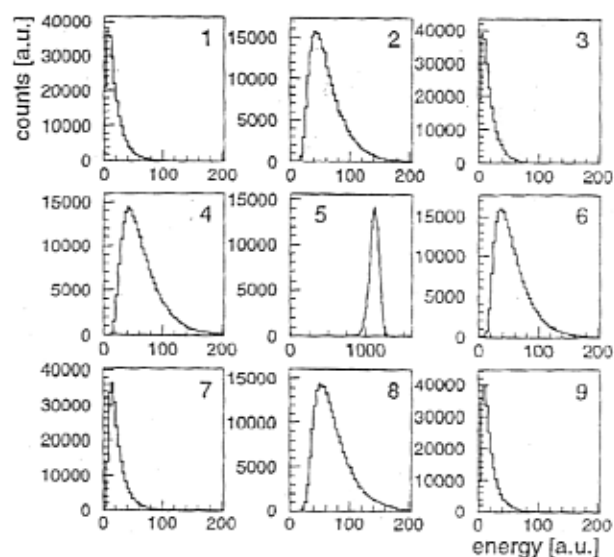


Figure 8: Response of the  $3 \times 3$   $\text{PbWO}_4$  matrix to electrons of 855 MeV energy shown in arbitrary units.

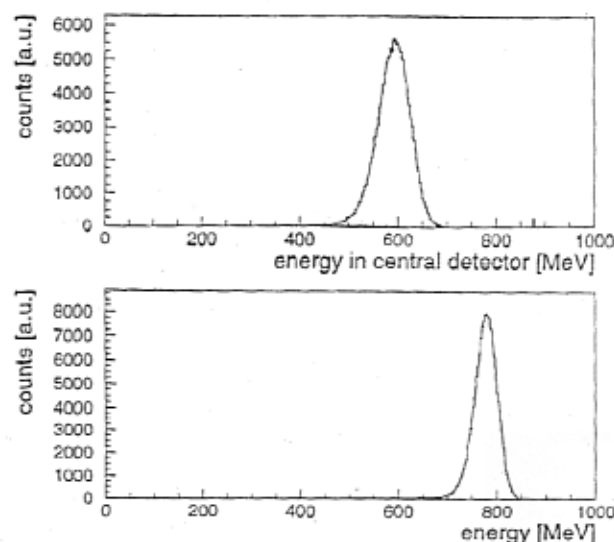


Figure 9: Energy response to 855 MeV electrons observed in the central module and the total  $\text{PbWO}_4$  crystal matrix, respectively. The detectors have been operated at a temperature of  $T = 2.5^\circ\text{C}$ . The absolute calibration is taken from GEANT3 (see chapter IV).

### C. The Energy and Position Response

The signal shape of each crystal - slightly modified due to the long coaxial cable - has been measured using a fast digital scope (TEKTRONIX TDS 744A). Fig. 10 compares the observed line shapes of all 9 crystals initiated by 855 MeV electrons. The peak value of the signal amplitude drops down to 20% within 22 to 36 ns. In a detailed analysis, slow decay components ( $\tau > 100$  ns) can be identified in all crystals, which explains the substantial increase of the light output of the array by 23% when integrating over a time width of 220 ns instead of 60 ns.

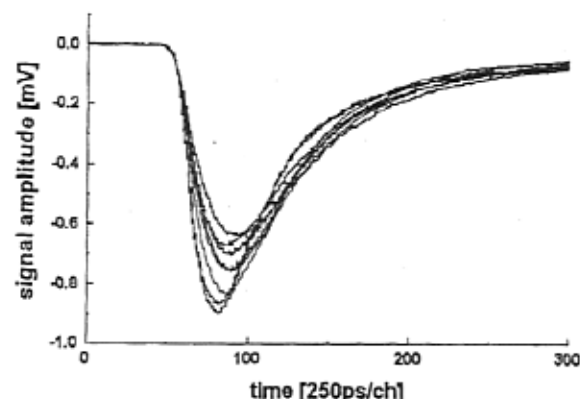


Figure 10: Line shape of the 9 PbWO<sub>4</sub> crystals initiated by 855 MeV electrons recorded with a digital scope. The signal amplitudes are arbitrarily normalized. 100 channels correspond to 25 ns on the horizontal time axis.

The measurement of the response of the crystals determined at the two different temperatures gives an increase of the integral light yield (LY) of 22% (IW = 140 ns) corresponding to a gradient of  $\Delta LY/\Delta T = -1.3\%/^{\circ}\text{C}$  at room temperature, which is below the typical value listed in literature (see Table 1). The energy resolution ( $\sigma/E$ ) can be directly taken from the measured response functions ( $\sigma = \text{FWHM}/2.355$ ). Fig. 11 illustrates as an additional example the achieved good resolution of  $\sigma/E = 5.83\%$  at the lowest investigated energy of  $E_c = 180$  MeV (IW = 220 ns). The dependence on the incident energy can be parameterized as (see Fig. 12)

$$\sigma/E = 2.39\% / \sqrt{E[\text{GeV}]} + 0.20\%.$$

The small Molière radius of PbWO<sub>4</sub> results in narrow showers as can be seen from the energy deposition in the central crystal. Nevertheless, the spread of the shower into the neighboring modules enables the measurement of the position of impact in spite of the strong shower fluctuations at incident energies below 1 GeV. The center of gravity can be calculated for both dimensions by  $X = (\Sigma_l - \Sigma_r) / \Sigma_{\text{tot}}$  (in a similar manner for Y). Here  $\Sigma_l$  and  $\Sigma_r$  refer to the sum over the weighted pulse heights in the columns of three crystals to the left and to the right of the central crystal and  $\Sigma_{\text{tot}}$  denotes the pulse height summed over all responding detectors. In order to

account for the transverse profile of an EM-shower the measured detector signals  $U_i$  ( $i=1,\dots,9$ ) are logarithmically weighted according to  $V_i = w + \log(U_i / \Sigma U_i)$ . Fig. 13 shows the reconstructed position distribution for a central point of impact measured at 855 MeV. The overall weighting factor has been set to  $w = 6$ . The achieved position resolution in both dimensions amounts to  $\sigma = 2.1$  mm ( $\sigma = 2.9$  mm at 180 MeV). The spot size defined by the requirement of a coincidence with the fiber cross has not been unfolded.

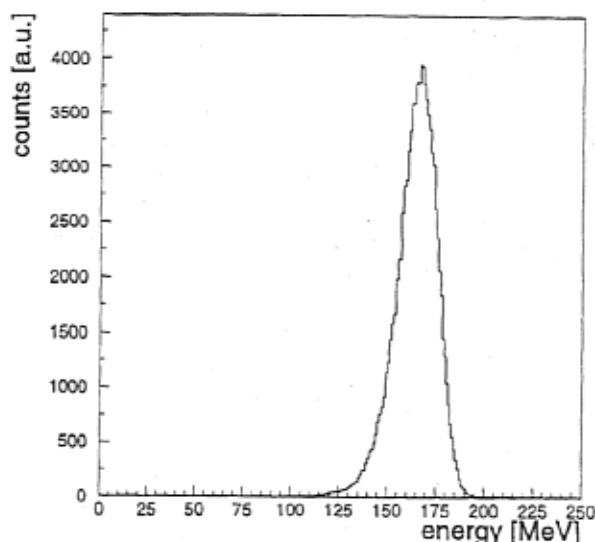


Figure 11: Energy response of the 3x3 PbWO<sub>4</sub> matrix to 180 MeV electrons. The crystals are operated at a temperature of  $T = 2.5^{\circ}\text{C}$ . The energy resolution amounts to  $\sigma/E = 5.83\%$ . The light output has been integrated over a width of 220 ns.

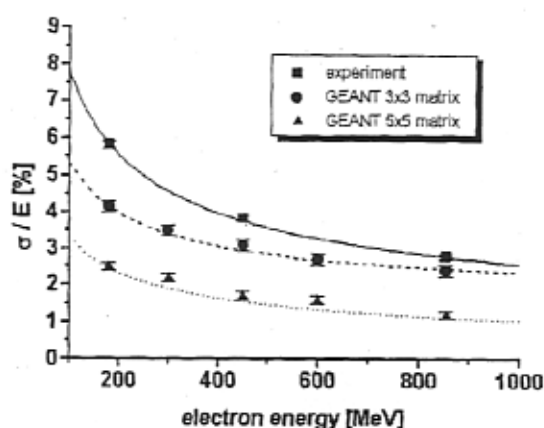


Figure 12: The experimental energy resolution of a 3x3 PbWO<sub>4</sub> crystal matrix shown as a function of the incident electron energy. GEANT3 simulations of two different detector arrangements are shown for comparison.

### D. The Time Response

The timing signal of each matrix component has been determined relative to the central detector. Similar pulse height

spectra can be obtained in two adjacent detector elements by positioning the beam between these modules. The distribution of the time difference of the response of the two detectors measured at  $E_e = 855$  MeV follows a Gaussian shape with a width of  $\sigma = 185$  ps. Assuming an identical behavior of each matrix element the experimental time resolution per detector reduces to  $\sigma = 185/\sqrt{2} \text{ ps} = 130 \text{ ps}$ .

#### IV. COMPARISON TO SIMULATIONS

The EM-shower initiated by electrons between 180 and 855 MeV has been simulated using the computer code GEANT3 [15]. The calculation takes only into account the crystal geometry and the energy loss due to dead material such as the PTFE reflector layer between adjacent crystals. The most probable value of the calculated deposited total energy has been used for an absolute calibration of the detector signals. The resolution of the simulated response function reflects the fluctuations of the shower and the leakage out of the finite active crystal volume. Fig. 12 shows the results obtained for a matrix of 3x3 crystals as used in the experiment as well as for a 5x5 matrix, respectively, in comparison to the experimental data.

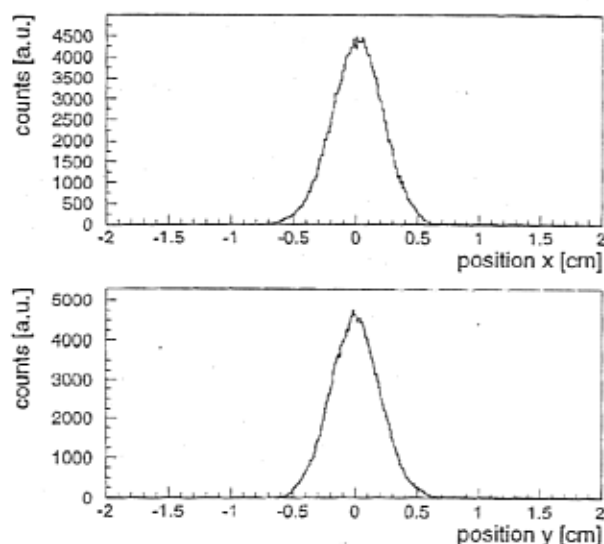


Figure 13: Distribution of the point of impact (the beam has been pointed onto the center of the matrix) reconstructed in two dimensions from the distribution of the electromagnetic shower. The measurement has been performed at the highest electron energy of 855 MeV. The algorithm is described in detail in the text.

#### V. DISCUSSION AND SUMMARY

Large  $\text{PbWO}_4$  crystals of depth  $> 16 X_0$  have been used to measure the response to monoenergetic electrons. The quality of the crystals has been characterized based on the optical transmission and the luminescence yield due to low energy  $\gamma$ -rays using hybrid photo diode tubes with high single photo-electron resolution. The samples perform in a very diverse

manner. Due to the small number of available crystals, no significant correlations can be established yet.

The line shape, energy and time resolutions of an array consisting of 9 crystals read-out by photomultipliers have been determined with monoenergetic electrons between 180 and 855 MeV energy. The used crystals show a strong scintillation component with decay times larger than 100 ns. This fact can limit the applicability in experiments with very high count rates causing pile-up.

The reconstruction of the EM-shower delivers good energy, position and time resolutions. In spite of the low scintillation yield of  $\text{PbWO}_4$ , a resolution value  $< 6\%$  has been achieved for the first time even at 180 MeV by operating the crystals at a reduced temperature ( $T = 2.5^\circ\text{C}$ ) and integrating the signal shape over a 220 ns wide time gate. The comparative study at two different temperatures ( $T = 2.5^\circ\text{C}$  and  $T = 20^\circ\text{C}$ ) at the highest incident energy of 855 MeV shows only a slight improvement of the energy resolution ( $\sigma/E = 3.0\%$  at  $T = 20^\circ\text{C}$ ) in spite of an increase of 22% of the recorded light yield. As illustrated by the performed GEANT3 simulations, the photon statistics of the scintillation light influences the energy resolution at low energies while shower leakage limits the results obtainable at 855 MeV. A larger active volume, such as a 5x5 crystal matrix, will substantially improve the resolution at energies below 1 GeV since the transverse leakage dominates in the used geometry. However, the large variation of the crystal performance gives hope, that in particular at energies of a few hundred MeV or lower an enhanced light output of selected and optimized crystals can bring the resolution value further down.

The obtained time resolution of  $\sigma = 130$  ps per module represents an upper limit even for the existing crystals since the timing signal has been derived after a long cable delay. Nevertheless, such a time resolution will allow particle/photon discrimination as required for example in relativistic heavy ion collisions when compact detector arrangements with a flight path even below 1 m become necessary to cover a sufficient solid angle.

As a conclusion, the detailed study has illustrated some new sensitive techniques for performance tests even considerable in case of large scale crystal productions, and has documented the new applicability of  $\text{PbWO}_4$  for photon calorimetry in reaction studies at medium or relativistic projectile energies.

#### VI. REFERENCES

- [1] R. Novotny, IEEE Trans. Nucl. Sci. 38 (1991) 379.
- [2] M. V. Korzhik et al., phys. stat. sol. (a) 154 (1996) 779.
- [3] P. Lecoq et al., Nucl. Instr. and Meth. in Phys. Res. A365 (1995) 291.
- [4] S. Inaba et al., Nucl. Instr. and Meth. in Phys. Res. A359 (1994) 485.
- [5] Yu. D. Prokoshkin et al., Nucl. Instr. and Meth. in Phys. Res. A362 (1995) 406.
- [6] J.P. Peigneux et al., Nucl. Instr. and Meth. in Phys. Res.

- A378 (1996) 410.
- [7] CMS Collaboration, Technical Proposal, CERN/LHCC 94-38.
  - [8] A Large Ion Collider Experiment, Technical Proposal, CERN/LHCC 95-71.
  - [9] RI&NC, Minsk, Republic of Belarus and Bogoroditsk Techno Chemical Plant, Russia.
  - [10] Shanghai SICCAS High Technology Corporation, Shanghai, China
  - [11] R. DeSalvo et al., Nucl. Instr. and Meth. in Phys. Res. A315 (1992) 375.
  - [12] H. Arnaudon et al., Nucl. Instr. and Meth. in Phys. Res. A342 (1994) 558.
  - [13] G. Anzivino et al., Nucl. Instr. and Meth. in Phys. Res. A365 (1995) 76.
  - [14] in collaboration with F. Maas, S. Koebis et al., Institute for Nuclear Physics, University Mainz, Germany.
  - [15] R. Brun et al., GEANT3, CERN/DD/cc/84-1.